Experimental analysis of H_3- and D_3-molecule autoionization

V. Berardi, N. Spinelli, and R. Velotta
Dipartimento di Scienze Fisiche, Università di Napoli, Padiglione 20, Mostra d'Oltremare, I-80125 Napoli, Italy

M. Armenante
Istituto Nazionale di Fisica Nucleare, Sezione di Napoli, I-80125 Napoli, Italy

A. Zecca
Dipartimento di Fisica, Università di Trento, 38050 Pantè di Povo (TN), Italy
(Received 9 April 1992)

Excited neutral triatomic hydrogen and deuterium molecules formed by electron-impact excitation have been investigated. We report on the autoionization of H_3^* and D_3^* molecules produced by the reactions $H_2^+ + H_2 \rightarrow H_3^* + H^+$ and $D_2^+ + D_2 \rightarrow D_3^* + D^+$. We measured the lifetime of H_3^* and D_3^* and the branching ratio between H_3^*, D_3^*, and H_3^+, D_3^+ production channels.

PACS number(s): 34.80.Gs, 34.90.+q

I. INTRODUCTION

The triatomic molecules H_3 and D_3 have been the subject of a great deal of theoretical and experimental investigations, due to the fact that they are the simplest polyatomic molecules. They are of considerable interest as a collision complex formed in the exchange reactions. H_3^+ is also of noticeable astrophysical interest because it is the most abundant ion in interstellar clouds.

H_3 and D_3 are molecular species that exist only in Rydberg excited states, the electronic ground state being repulsive. The H_3 and D_3 long-lived highly excited states are of great importance when considering the energetic balance of plasma systems, while the triatomic ion H_3^+ is the major charge carrier in hydrogen discharges.

The existence of a long-lived H_3 molecule was experimentally evidenced by Devienne [1] through a neutralized-ion-beam technique. Later on, through the same technique, Nagasaki *et al.* [2] performed a similar analysis on D_3. Unfortunately, they were able to estimate only the lower limit of the lifetime of the neutral triatomic molecule (100 ns), without any distinction between dissociation and autoionization. Metastable H_3 molecules have also been observed by Garvey and Kuppermann [3], who estimated the lower limit of the lifetime of the states they populated to be 40 μs. However, they could not observe any decay faster than 1 μs.

The production of H_3 and D_3 was then obtained in hollow cathode gas discharges by Herzberg and co-workers [4–7] who studied the emission spectra of these molecules. Bands in the visible and infrared ranges were analyzed and the interpretation of these spectra showed that neutral triatomic molecules H_3 and D_3 can be considered as Rydberg molecules with one electron orbiting around the ionic core (H_3^+ and D_3^+).

The neutralized mass selected ion beam technique has been used by Figger and co-workers for spectroscopic of H_3 and D_3 molecules [8–11]. By using such a technique Helm and co-workers [12–14] studied the H_3 high-n Rydberg states, excited from long-lived levels, showing the existence of a series of autoionizing transitions converging to vibrationally excited or vibrationless states of H_3^+, although neither the lifetimes of the excited molecules nor their production cross sections were investigated. Dodhy *et al.* [15] analyzed the irregularities in the intensity of the emission lines, pointing out the importance of nonradiative processes in the H_3 molecule. They were able to show that the lifetime of states with $14 \leq n \leq 65$ covers a wide range, although it was impossible to extract accurate lifetimes from their measurements.

In this paper we report on the formation of $H_3^*(D_3^*)$ as a collision complex, measuring the lifetime of their autoionizing states decaying in $H_3^+(D_3^+)$, produced by electron impact. We have investigated the reactions $H_2^+ + H_2 \rightarrow H_3^* + H^+$ and $D_2^+ + D_2 \rightarrow D_3^* + D^+$; the produced $H_3^*(D_3^*)$ molecule has been found to have a long lifetime and a very high production cross section.

II. EXPERIMENT

A. General

In this subsection we will describe the main features of the experimental setup, devoting next subsection to a detailed description of the electronic chain we used.

The apparatus, schematically depicted in Fig. 1, essentially consists of a linear time-of-flight (TOF) spectrometer. The investigated species, produced by a pulsed electron beam, are extracted from the interaction region by a pulsed electric field.

In order to measure the lifetime of long-lived autoionizing molecules and their production cross section, we analyzed the dependence of the time-of-flight distribution of the investigated species from the delay between the rise of the electron pulse and the rise of the extraction field.

In the interaction region a stainless steel needle injector ($\phi = 100$ μm), fed by a variable, programmable, self-controlling leak (Granville-Phillips mod.216), provides

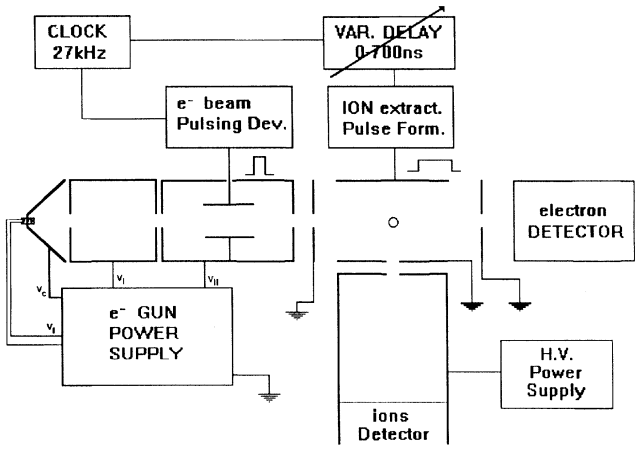

FIG. 1. Schematic of the experimental apparatus.

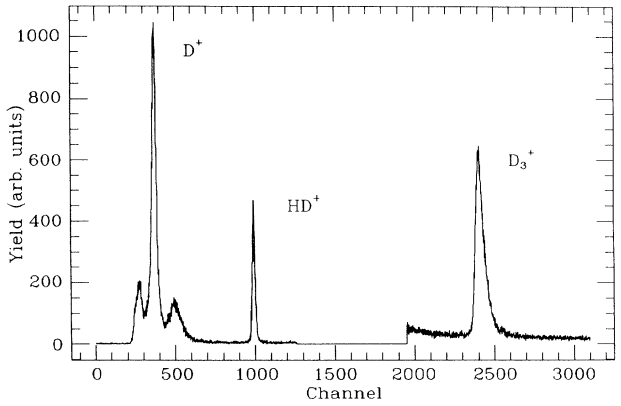

FIG. 2. TOF spectrum of D_2 molecules. The blank region corresponds to parent ions (D_2^+) that are not timed to avoid MCA pileup.

for the continuous inflating of the gas sample.

The target molecules interact with a pulsed electron beam (peak intensity $\sim 10^{-5}$ A, pulse length 40 ns, electron energy 100 eV), produced by an electron gun, and the resulting ions are drawn from the source at right angles with respect to both the electron gun axis and the gas beam direction. The extraction voltage is switched on with a variable delay $R(0-700$ ns) with respect to the end of the electron pulse.

After being extracted, the ions enter the acceleration region and then the field-free region, at the end of which they are detected. The combination of electric fields has been chosen in order to both obtain a negligible TOF dependence on the ion impact point over the detector and to minimize the TOF spread of the ions due to different initial positions (spatial focusing). We used in this work the same detection system as in [16]; it essentially consists of an assembly of a multichannel plate and a 14-focusing-dynode electron multiplier. The whole apparatus is contained in a high-vacuum cylindrical chamber (400 mm inner diameter), pumped down to 4×10^{-9} torr. The local pressure in the ionization region was estimated to be ~ 100 times the pressure reading in the vacuum chamber.

The TOF spectrometer has been set to operate in a spatial focusing mode; in this condition two ions form with the same kinetic energy, but different positions, have almost the same TOF; thus the width of the TOF distributions can be essentially ascribed to the ion kinetic energy spread. Since the origin of TOF's is the instant at which the extraction field switches on, the electron pulse length does not affect the TOF distributions.

The optimum spatial focusing condition corresponds to a well-defined value of the ratio between the extraction and the acceleration field; the values were experimentally found by varying the extraction and the acceleration field to minimize the ratio between the TOF distribution width of a selected ion and the time interval between peaks corresponding to different species. We performed this procedure by analyzing the HD^+ distribution in the D_2 TOF spectrum. The HD molecule is present in traces in the D_2 gas cylinder, and HD^+ ions are formed with thermal kinetic energy; this makes the HD^+ TOF distribution very narrow and symmetric. In Fig. 2, a complete TOF spectrum of electron-impact ionization of deuterium molecules is shown.

B. Electronic chain

In order to measure the TOF of species whose abundances are different by several orders of magnitude, the electronic hardware sketched in Fig. 3 has been realized. We find it convenient to adopt the inverted timing method by using the ion detector signal as the start pulse for the time-to-amplitude converter (TAC) and a properly delayed signal as the stop. In fact, in this way we can choose to time only *single events;* that is, we reject events belonging to cycles in which more than one ion lets the detector produce a signal. Multiple ion rejection is real-

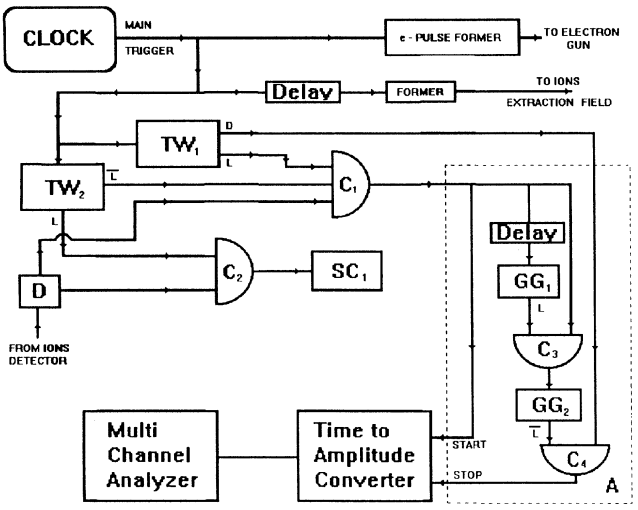

FIG. 3. Electronic chain: GG, gate generator; D, discriminator; Sc, scaler; C, coincidence unit; TW, time window unit; ID, ion detector; MCA, multichannel analyzer; TAC, time-to-amplitude converter.

ized by box A of the electron chain of Fig. 3. The first signal from the detector enables the C_1 coincidence; if another ion is detected, its signal triggers the gate generator GG_2, disabling C_4, to prevent the stop signal from reaching the time-to-amplitude converter.

As is well known, the time inverted technique is very efficient when the mean rate N of detected particles per cycle is ~ 0.2 [17,18]. In our working conditions the production of parent ions is so high that $N > 1$; this means that the simple single shot operation does not work for parent ions because the probability of detection of more than one particle per cycle is very high. Therefore an analogic technique would seem more appropriate, at least for parent ions. Unfortunately the abundance of all the other ions, which are only a small fraction of the parents, is too low for using analogic techniques.

In this intermediate regime, in which neither counting technique nor analogic one works in a satisfactory way, we are compelled to look for a compromise. Since we are not interested in the peak shape of the patent ion, we simply count them, disabling the TAC in the time interval corresponding to the arrival of the parent ions.

Referring to Fig. 3 we see that the time window TW_2 enables C_2 or C_1. In the first case the signal coming from the ion detector ID is only counted, whereas in the second case the signal is sent to the multichannel analyzer (MCA) for timing. The time window TW_1 is the interval in which events are accepted by the TAC-MCA system.

The resulting TOF spectrum for D_2 molecules has been shown in Fig. 2 in which the blanking corresponding to parent ions is clearly visible. The measured time resolution is 1.1 ns/channel.

The TOF peak of the triatomic molecule (either H_3^+ or D_3^+) has been found to be strongly nonsymmetric. In particular, there is a pronounced tail corresponding to particles either electrically neutral at the extraction field switching on, becoming charged later on, or coming from collisions involving neutral species. In fact, the ions present in the source when the extraction field is switched on give rise to symmetric TOF distribution. Therefore the analysis of TOF distribution as a function of the delay introduced between the electron pulse and the extraction field allows us to obtain quantitative information about the characteristic times of ion production through processes involving neutral long-lived species. In the following we shall examine all the processes that could influence the shape of the time distribution, in order to take into account their relative importance.

III. DATA ANALYSIS

Charged molecules M_3^+ (henceforth M will be used to indicate H or D) are produced via the following reactions:

$$M_2^+ + M_2 \rightarrow M_3^+ + M \ , \tag{1}$$

$$M_2^* + M_2 \rightarrow M_3^+ + M^- \ , \tag{2}$$

$$M_2^* + M_2 \rightarrow M_3^+ + M + e^- \ , \tag{3}$$

$$M_2^* \rightarrow M^* + M \ , \tag{4}$$

$$M^* + M_2 \rightarrow M_3^* + e^- \ , \tag{5}$$

$$M_2^+ + M_2 \rightarrow M_3^* + M^+ \ , \tag{6}$$

$$M_3^* \underset{\tau}{\rightarrow} M_3^+ + e \ , \tag{7}$$

τ being the lifetime of M_3^*. Concerning hydrogen, the cross section for the reaction (1) is estimated to be $\sim 80 \times 10^{-16}$ cm^2 [19]. In [20] it has been shown that the production of H_3^+ through the reactions (4) and (5) is negligible with respect to that occurring through reaction (1) due to the very low value of the cross section for reaction (5) ($\sim 10^{-16}$ cm^2), even for the long-lived (0.142-sec) H($2s$). Moreover, the cross section for the formation of H_2^+ at an electron-impact energy of 100 eV (0.8×10^{-16} cm^2) is larger than that for the formation of H_2^* ($< 0.5 \times 10^{-16}$ cm^2) [21].

As previously evidenced, when the apparatus operates in a spatial focusing condition, all the particles that are charged when the extraction field switches on do produce TOF distributions that are symmetric in shape. In Fig. 4(a) the TOF distribution of HD^+, which comes solely from primary processes, is shown; it is evident that the symmetry and the width are conserved, even after introducing the delay.

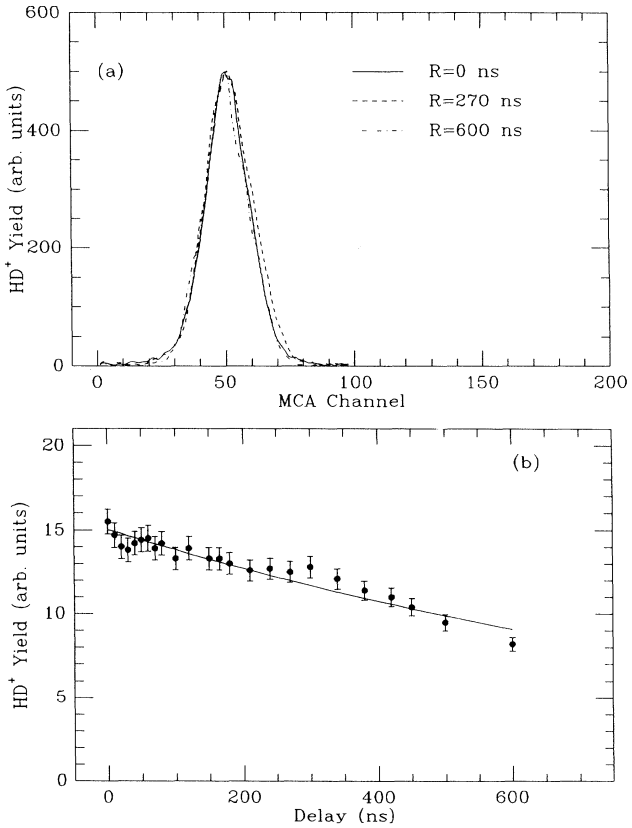

FIG. 4. (a) HD^+ peaks for various delays between the extraction field switching on and the electron pulse. The symmetry and the width of the peaks are not influenced by the introduction of the delay. (b) Ionic yield vs delay R for HD^+ ions. The full line curve follows an exponential law of time constant $\tau \sim 1200$ ns.

Therefore, the tail at longer times is entirely due to triatomic ions, formed after the extraction field has switched on, and through reactions (2), (3), and (7).

The reactions (2) and (3) give a tail at the TOF distribution longer time, with a time constant of the order of the characteristic time of collisional processes. To give an estimation of such a time we evaluate the collision frequency (ν) in the source. We have

$$\nu = N\sigma v \ , \tag{8}$$

where N is the density of the species, σ is the cross section, and v the relative velocity between the colliders. Inserting the value of N corresponding to a pressure $P = 10^{-2}$ torr, $\sigma = 100$ Å^2 [corresponding to reaction (1) which has the highest cross section] and $v \sim \sqrt{kT/m}$, we obtain

$$\nu \ll \frac{10^6}{\sqrt{m}} \ \mathrm{s}^{-1} \ , \tag{9}$$

where m is in amu.

Therefore for any process due to collisions the following relation holds:

$$\tau_{\mathrm{coll}} \gg \sqrt{m} \ \mu\mathrm{s} \ . \tag{10}$$

From Fig. 5 we see that the characteristic time of the M_3^+ peak tail is of the order of ~ 100 ns, whereas Eq. (10) gives a time much larger than 1.4 μs for H_2 and 2.0 μs for D_2 molecules. It is expected that the same arguments about the relative importance of reactions (1)–(5) hold true for the deuterium too. To evaluate the branching ratio, the reactions (1) and (6), and the lifetime of M_3^*, we analyzed the M_3^+ production as a function of the delay introduced between the end of electron pulse and the extraction field switching on.

In Fig. 5 the peaks of D_3^+ recorded at different delays and normalized to their maximum are shown. There is a remarkable change in the peak shape: the side tail at longer time clearly decreases when the delay increases, while the short-time side tail is almost unaffected by the delay.

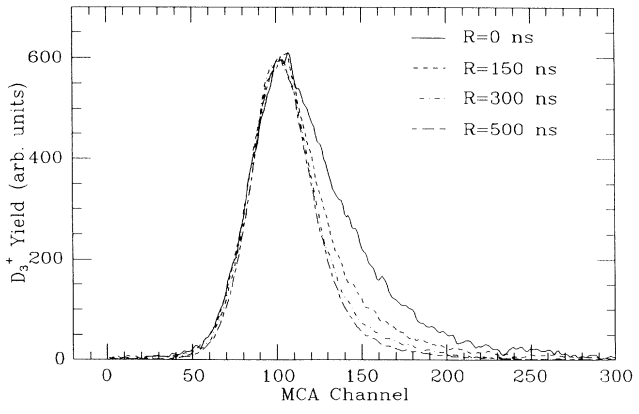

FIG. 5. D_3^+ peaks recorded for various delays between the extraction field switching on and the electron pulse (normalized to the maximum).

A detailed analysis requires one to examine the processes leading to M_3^+ losses. The major competing processes for M_3^+ production can be assumed to be the diffusion of both M_2 and $M_3^+(M_3^*)$ and the recombination processes of M_3^+.

Diffusion

Diffusion loss has been investigated by using the HD^+ peak and measuring its yield and its width as a function of delay, as shown in Figs. 4(a) and 4(b). The decrease of HD^+ yield due to the diffusion is clearly visible in Fig. 4(b). The time scale of this process can be obtained by fitting the experimental points by an exponential law, as shown in the same figure. The time constant obtained is $\tau_{\mathrm{diff}} \sim 1200$ ns, and we expect $\tau_{\mathrm{diff}} \propto m$ if collisions are predominant, whereas $\tau_{\mathrm{diff}} \propto \sqrt{m}$ if the expansion can be considered free. Our working pressure justifies the latter approximation; therefore, the characteristic times of the diffusion of H_2^+ and D_2^+ are ~ 980 and ~ 1400 ns, respectively; these values are larger than the characteristic of the M_3^+ peak tail. Of course for ionic triatomic molecules this argument holds even more. Figures 6(a) and 6(b) show that the diffusion is negligible up to 200 and 400 ns for H_3^+ and D_3^+, respectively, and is responsible of the plateau occurring at larger values of the delay.

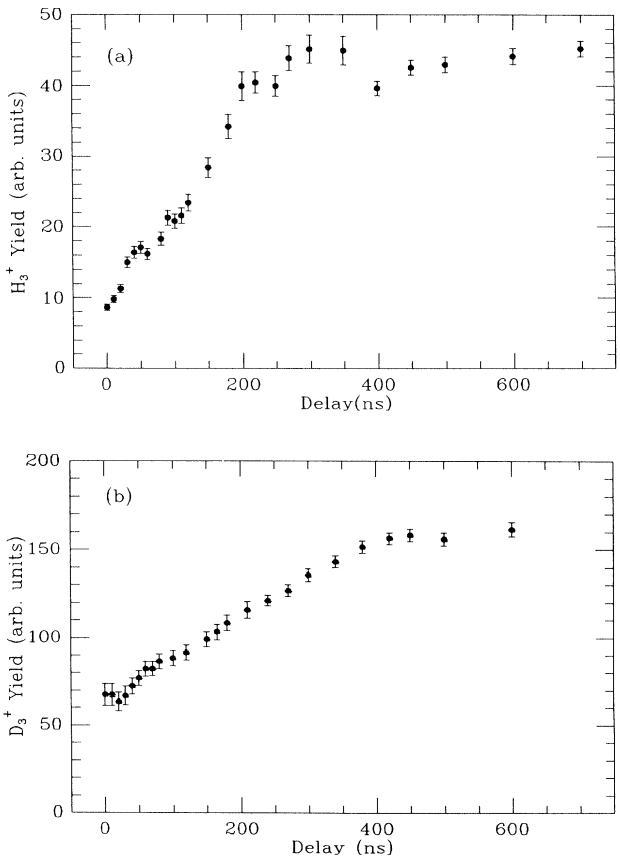

FIG. 6. Ionic yield vs delay R for (a) H_3^+; (b) D_3^+.

Electron collision of M_3^+

The dissociative recombination of M_3^+,

$$e+M_3^+ \rightarrow M_2+M \ , \tag{11}$$

$$\rightarrow M+M+M \ , \tag{12}$$

is the major neutralization processes for M_3^+ [22,23]. The cross section for this process strongly depends on the relative velocity between electron and ion. For hydrogen its highest value is $\sim 10^{-13}$ cm^2, corresponding to a null center-of-mass energy, and it decreases to $\sim 10^{-16}$ cm^2 as the center-of-mass energy reaches 1 eV. Concerning deuterium the cross section is even smaller in this range.

Studies on dissociative excitation of H_3^+ [24],

$$e+H_3^+ \rightarrow H+H_2^+ +e \ , \tag{13}$$

$$\rightarrow H_2+H^+ +e \ , \tag{14}$$

showed that the cross section for these processes exhibits resonances but never exceeds 10^{-16} cm^2.

The recombination channel,

$$e+H_3^+ \rightarrow H_3^* \ , \tag{15}$$

has been found to constitute only about 8% of the total recombination processes [sum of processes (11), (12), and (15)] [25]. The above given cross sections for recombination lead to a completely negligible collision frequency among triatomic ions and both secondary and primary electrons. In fact, for the processes that involve secondary electrons, the produced charge density is $\sim 10^7$ cm^{-3} and the cross section for recombination can be assumed to be $\sim 10^{-13}$ cm^2; thus inserting these values into Eq. (8) we get the characteristic time for recombination, $T_{\rm rec} \gg 1$ msec. If we consider collisions between the triatomic ion and primary electrons the low value of the cross section produces a recombination time even larger.

Recapitulating, we have the following channels that could influence the production rate of M_3^+ by introducing a delay between the end of electron pulse and the extraction field switching on: (a) diffusion of reactants M_2^+ and M_2; (b) diffusion of M_3^+; (c) decrease of the reactants due to the production of M_3^+; (d) decay of M_3^* due to secondary collision; and (e) recombination.

For each of the processes (a)–(e) we have a characteristic time scale larger than the time range in which we shall carry on the analysis. Thus we can assume (1) the density of reactants to be almost constant during the delay, and hence a linear dependence of the total M_3^+ yields on the delay as it is seen in Figs. 6(a) and 6(b); and (2) that the width reduction of the M_3^+ peak as a function of the delay cannot be ascribed to any process other than the decay of M_3^*.

IV. RESULTS AND DISCUSSIONS

The time-of-flight distribution corresponding to the triatomic mass includes ions present in the interaction region at the extraction field switching on ($\mathcal{M}_3^+{}_0$) and ions produced later on through the decay of $\mathcal{M}_3^*$ ($\mathcal{M}_3^*{}_{nd}$); that is,

$$\mathcal{M}_3^+{}_{\rm tot}(R)=\mathcal{M}_3^+{}_0(R)+\mathcal{M}_3^*{}_{nd}(R) \ . \tag{16}$$

The former ions give rise to a symmetric peak that is well approximated by a Gaussian law, whereas the TOF distribution of the latter ones is given by the following convolution:

$$\frac{1}{\sqrt{\pi}\sigma\tau}\int_0^\infty dx \exp\left\{-\frac{(x-t)^2}{\sigma^2}\right\}\exp\left\{-\frac{x}{\tau}\right\} , \tag{17}$$

where σ is the width of the symmetric peak.

To evaluate the cross section of reaction (7) and the lifetime of M_3^*, we measured the ratio between the total area of the peak ($\mathcal{M}_3^+{}_{\rm tot}$) and the area of a selected number of channels around the maximum. We chose for both hydrogen and deuterium a time interval (Δt) of seven channels, corresponding to 7.7 ns with our resolution. In these channels the main contribution comes from ions already formed when the extraction field is switched on, whereas a smaller contribution comes from the decay of $\mathcal{M}_3^*{}_{nd}(R)$ occurring during Δt. The fraction of $\mathcal{M}_3^*{}_{nd}$ decaying in the interval Δt is immediately obtained by integrated the TOF distribution (17). Assuming $\Delta t \ll \sigma \ll \tau$, it is easy to show that

$$\frac{1}{\sqrt{\pi}\sigma\tau}\int_{-\Delta t/2}^{\Delta t/2} dt \int_0^\infty dx \exp\left\{-\frac{(x-t)^2}{\sigma^2}\right\}\exp\left\{-\frac{x}{\tau}\right\}\approx\frac{\Delta t}{2\tau} \ . \tag{18}$$

We shall indicate as $1/\phi$ the ratio between total area of the peak and the area corresponding to an interval Δt around the maximum when decay phenomena are absent and the peak is symmetric. Therefore, the measured quantity is given by

$$\frac{\mathcal{M}_3^+{}_{\rm tot}}{\phi\mathcal{M}_3^+{}_0+\dfrac{\Delta t}{2\tau}\mathcal{M}_3^*{}_{nd}}=\frac{1}{\phi(1-\mathcal{M}_3^*{}_{nd}/\mathcal{M}_3^+{}_{\rm tot})+\dfrac{\Delta t}{2\tau}(\mathcal{M}_3^*{}_{nd}/\mathcal{M}_3^+{}_{\rm tot})} \ . \tag{19}$$

Reactions (1) and (7) give a quadratic dependence of both M_3^+ and M_3^* on the electron pulse length T. Since the reactants are the same for all the reactions and their velocity is very small (thermal), we have $\langle \sigma^+ v \rangle \sim \sigma^+ \langle v \rangle$ and $\langle \sigma^* v \rangle \sim \sigma^* \langle v \rangle$. Therefore,

$$\mathcal{M}_3^+{}_{\rm tot}(0)=\tfrac{1}{2}(\sigma^+ +\sigma^*)\alpha T^2 \ , \tag{20}$$

where $\alpha = k\langle v \rangle n^2$, k is the rate of reaction $e+M^2 \rightarrow M_2^+ +e+e$, and n is the gas density.

According to what was stated in the previous section,

during the delay we can assume the M_2^+ density to be constant in the time scale of our analysis; thus we expect a linear dependence of $M_3{}^+_{\rm tot}$ on the delay R. Figures 6(a) and 6(b) confirm the above assumptions for hydrogen and deuterium, respectively. Therefore, we can write

$$\mathcal{M}_3{}^+_{\rm tot}(R)=\mathcal{M}_3{}^+_{\rm tot}(0)+\beta(\sigma^+ +\sigma^*)R \ , \tag{21}$$

where $\beta=\langle v\rangle\gamma n^2$, and $\gamma\equiv[M_2^+]/[M_2]$ is the ionization ratio.

Using (20) and (21) we can write the total collected ionic triatomic molecules as

$$\mathcal{M}_3{}^+_{\rm tot}(R)=(\sigma^+ +\sigma^*)(\tfrac{1}{2}\alpha T^2+\beta R) \ . \tag{22}$$

The fraction $\mathcal{M}_3{}^*_{nd}(R)$ of molecules not decayed at the instant R, when the extraction field is switched on, is given by the following rate equation:

$$\frac{d\mathcal{M}_3{}^*_{nd}}{dt}=H(t)-\frac{\mathcal{M}_3{}^*_{nd}}{\tau} \ , \tag{23}$$

where $H(t)$ is the production rate of $M_3{}^*$. According to the assumptions that have led us to relations (20) and (21), we have $H(t)=\alpha\sigma^* t$ during the electron pulse, and $H(t)=\beta\sigma^*$ during the delay R. The integration of (23) gives

$$\mathcal{M}_3{}^*_{nd}(R)=\sigma^*\alpha\tau[T-\tau(1-e^{-T/\tau})]e^{-R/\tau} +\sigma^*\beta\tau(1-e^{-R/\tau}) \ . \tag{24}$$

The factor $\sigma^*\alpha\tau[T-\tau(1-e^{-T/\tau})]$ in the first term of Eq. (24) is relative to $M_3{}^*$ molecules produced during the electron pulse T and not yet decayed. The second term describes the production and the decay during the delay R. By setting

$$\kappa=\frac{\sigma^*}{\sigma^+} \ , \tag{25}$$

we have

$$\frac{\mathcal{M}_3{}^*_{nd}}{\mathcal{M}_3{}^+_{\rm tot}}=\frac{\kappa\alpha\tau[T-\tau(1-e^{-T/\tau})]e^{-R/\tau}+\kappa\beta\tau(1-e^{-R/\tau})}{(\sigma^+ +\sigma^*)(\frac{1}{2}\alpha T^2+\beta R)} \ . \tag{26}$$

Using the linear dependence of the rate on the delay, we fitted the experimental data by the function $\mathcal{M}_3{}^+_{\rm tot}(R)=aR+b$, and from Eq. (22) we obtain

$$\frac{b}{a}=\frac{\alpha T^2}{2\beta}\equiv F \ . \tag{27}$$

By simple algebra we get

$$\frac{\mathcal{M}_3{}^*_{nd}}{\mathcal{M}_3{}^+_{\rm tot}}=\frac{\left[\kappa F\dfrac{2\tau}{T}\right]\left[1-\dfrac{\tau}{T}(1-e^{-T/\tau})\right]e^{-R/\tau}+\kappa\tau(1-e^{-R/\tau})}{(1+\kappa)(F+R)} \ . \tag{28}$$

Inserting (28) in (19) we can relate our experimental data to the three unknown parameters κ, τ, and ϕ, we minimized the χ^2 function with respect to κ, τ, and ϕ; the fitting curves are shown in Figs. 7(a) and 7(b), while the values obtained for the parameters are given in Table I.

The measurements for deuterium were repeated at a lower pressure ($P=6.5\times10^{-5}$ torr background pressure), as shown in Fig. 7(c); the experimental points are more scattered because of the worse statistic, but the agreement with the high-pressure analysis is very satisfactory.

The values of the obtained lifetimes justify the approximations previously discussed. In fact, as stated above, $\tau_{H_3^*}$ and $\tau_{D_3^*}$ are much smaller than time scales of collisions and diffusion of both the reactants and the products. This allows us to conclude that the effect we are considering is due neither to diffusion nor to secondary collisions of $M_3{}^*$, but to one or more autoionizing states of $M_3{}^*$ produced through reaction (7).

The value of the lifetime we have found is to be considered an average of the lifetimes of several high-lying Rydberg states weighted by the probability of populating those states. Therefore, our measurements show that states whose lifetime is longer than 100 ns are scarcely populated in our pressure condition. Long-lived states whose lifetime is $\gg$500 ns, observed by other authors [3], could not be analyzed by our experimental setup because of diffusion. However, we are able to neglect their contribution to our measurements; in fact, molecules produced in such states would give rise to a tail much longer than the one observed in Fig. 4 for a null delay.

In Ref. [2] the lower limit of 100 ns for the D_3 lifetime was found. This is consistent with the more precise value

TABLE I. Branching ratio k, lifetime τ, and ϕ parameter obtained for hydrogen and deuterium.

	Hydrogen	Deuterium
$\sigma_{M_3^*}/\sigma_{M_3^+}$	0.48±0.07	1.03±0.05
$\tau_{M_3^*}$ (ns)	101±25	261±10
$\phi_{M_3^+}$	0.214±0.003	0.175±0.001

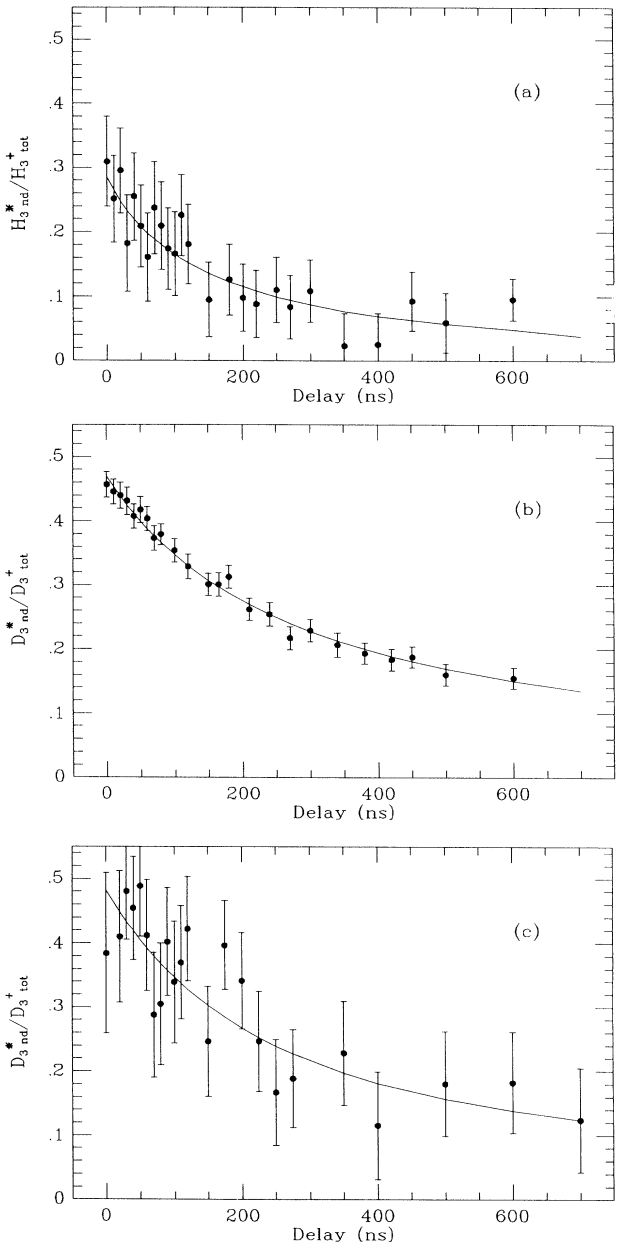

FIG. 7. Ratio between long-lived triatomic molecules present in the source at the extraction field switching on ($\mathcal{M}_3{}^*{}_{nd}$) and the total collected charge $\mathcal{M}_3{}^+{}_{tot}$ for (a) $H_3{}^+(P=9.2\times10^{-5}$ torr); (b) $D_3{}^+(P=9.6\times10^{-5}$ torr; (c) $D_3{}^+$ $(P=6.5\times10^{-5}$ torr). ● experimental points; full line, result of the fit.

we have obtained. This value is much larger than that found for $H_3{}^*$ due to the isotopical effect. This effect can be explained by invoking the different rotovibronic structure of $H_3{}^+$ and $D_3{}^+$ cores, affecting the stability of Rydberg states formed via reaction (7).

Dodhy *et al.* [15] gave an estimation of the lifetime of long-lived, high-n Rydberg states of $H_3{}^*$. From their analysis they could argue that there are states whose lifetimes range from less than 100 ns to more than 300 ns. A comparison with our results shows that nonradiative decays have to be taken into account for these states. Finally the ratios of cross sections for production of $M_3{}^+$ [reaction (1)] and $M_3{}^*$ [reaction (7)] are estimated. The values for the branching ratio k have been found to be 0.48 ± 0.07 for hydrogen and 1.03 ± 0.05 for deuterium.

These high branching-ratio values for the production of triatomic ion through the excited states of the triatomic molecule, indicate a non-negligible production of long-lived species. The considerably high values for the relative cross section we have found allow us to say that the autoionizing states of $H_3{}^*$ and $D_3{}^*$ play an important role in the evolution of hydrogenic plasmas. In fact, when the molecular dynamic of such plasmas is observed in time scales of the order of the lifetimes of the triatomic excited molecules, it must be taken into account that the production of the triatomic ion occurs through two channels: (i) direct production of triatomic ion via reaction (1); and (ii) production of triatomic excited molecules, which decay via reaction (7).

V. CONCLUSIONS

We report on the study of $H_3{}^*$ and $D_3{}^*$ molecule formation as an intermediate collision complex in the electron-impact production of $H_3{}^+$ and $D_3{}^+$. The production cross sections relative to $H_3{}^+$ and $D_3{}^+$, respectively, were also evaluated. They have been found to be 0.48 ± 0.07 for hydrogen and 1.03 ± 0.05 for deuterium, respectively. By time-of-flight measurements the lifetimes of the excited collision complexes have been evaluated to be 101 ± 25 for $H_3{}^*$ and 261 ± 10 ns for $D_3{}^*$.

We found considerably high values of the branching ratio k, for the production of the triatomic ion; as a consequence the autoionizing states of $H_3{}^*$ and $D_3{}^*$ play an important role in the solution of hydrogenic plasmas.

ACKNOWLEDGMENTS

The authors are pleased to acknowledge the technical assistance of Antonio Anastasio throughout this work. This research was partially supported by the Consiglio Nazionale delle Ricerche under the Progetto Strategico Clima, Ambiente e Territorio nel Mezzogiorno, and by INO.

[1] M. F. Devienne, Acad. Sci. **B267**, 1279 (1968).
[2] T. Nagasaki, H. Doi, K. Wada, K. Higashi, and F. Fukuzawa, Phys. Lett. **38A**, 381 (1972).
[3] J. F. Garvey and A. Kuppermann, Chem. Phys. Lett. **107**, 491 (1984).
[4] G. Herzberg, J. Chem. Phys. **70**, 4806 (1979).
[5] I. Dabrowski and G. Herzberg, Can. J. Phys. **58**, 1238 (1980).
[6] G. Herzberg and J. K. G. Watson, Can. J. Phys. **58**, 1250 (1980).
[7] G. Herzberg, H. Lew, J. J. Sloan, and J. K. G. Watson, Can. J. Phys. **59**, 428 (1981).
[8] H. Figger, M. N. Dixit, R. Mayer, W. Schrepp, H. Walther, I. R. Peterkin, and J. K. G. Watson, Phys. Rev. Lett. **52**, 906 (1984).
[9] H. Figger, Y. Fukuda, W. Ketterle, and H. Walther, Can. J. Phys. **62**, 1274 (1984).
[10] H. Figger, W. Ketterle, and H. Walther, Z. Phys. D **13**, 129 (1989).
[11] W. Ketterle, H. Figger, and H. Walther, Z. Phys. D **13**, 139 (1989).
[12] H. Helm, Phys. Rev. Lett. **56**, 42 (1986).
[13] H. Helm, Phys. Rev. A **38**, 3425 (1988).
[14] L. J. Lembo, A. Petit, and H. Helm, Phys. Rev. A **39**, 3721 (1989).
[15] A. Dodhy, W. Ketterle, H. P. Messmer, and H. Walther, Chem. Phys. Lett. **151**, 133 (1988).
[16] G. Arena, M. Armenante, S. Salerni, and N. Spinelli, Rapid Commun. Mass Spectrom. **2**, 35 (1988).
[17] P. B. Coates, Rev. Sci. Instrum. **43**, 1855 (1972).
[18] F. Esposito, V. Berardi, N. Spinelli, and R. Velotta, Rev. Sci. Instrum. **62**, 2822 (1991).
[19] D. Van Pijkeren, E. Boltjes, J. Van Eck, and A. Niehaus, Chem. Phys. **91**, 293 (1984).
[20] W. A. Chupka, M. E. Russel, and K. Refaey, J. Chem. Phys. **48**, 1518 (1968).
[21] H. Tawara, Y. Itikawa, H. Nishimura, and M. Yoshino, J. Phys. Chem. **19**, 617 (1990).
[22] B. Peart and K. T. Dolder, J. Phys. B **7**, 1567 (1974).
[23] J. B. A. Mitchell, C. T. Ng, L. Forand, R. Janssen, and J. W. McGowan, J. Phys. B **17**, L909 (1984).
[24] F. B. Yousif, P. J. T. Van der Donk, M. Orakzai, and J. B. A. Mitchell, Phys. Rev. A **44**, 5653 (1992).
[25] J. B. A. Mitchell and F. B. Yousif, in *Microwave and Particle Beam Sources and Directed Energy Concepts,* edited by H. E. Brandt (Optical Society of America, Washington, DC, 1989), Vol. 1061, p. 61.